

CHAPTER 2

Physics at GLC

Contents

2.1	Physics Goals of the GLC experiment	78
2.2	Higgs Physics	80
2.3	Direct Signals of New Physics	88
2.3.1	Supersymmetry	88
2.3.2	Large Extra Dimensions	94
2.4	Probing New Physics through Top Quark and Gauge Boson Processes	96
2.4.1	Physics with Top Quark	96
2.4.2	W Boson	98
2.5	Complementarity of LHC and GLC	99
2.6	Summary	102

2.1 Physics Goals of the GLC experiment

Elementary particle physics is a quest for the fundamental building blocks of the Universe and the forces acting between them. Progress in particle physics has been guided by new and often unexpected discoveries brought about by collider experiments. The operation of a new accelerator at a higher energy hence marks an opportunity to survey the laws of Nature at a more fundamental level.

High energy physics in the past three decades has been a success story for the so-called Standard Model. This is a theory that describes the strong, the electromagnetic and the weak interactions, which represent three of the four known fundamental forces, the fourth being gravity. This theory has two constituents: the “gauge principle” and the “Higgs mechanism”.

The gauge principle provides a unified picture of the three interactions in terms of the $SU(3) \times SU(2) \times U(1)$ gauge symmetry. The discovery of the gauge bosons that were postulated as the cause of these interactions, the W^\pm and the Z^0 , as well as the gluon, confirmed the validity of this gauge principle. The universality of the interaction strengths is another direct consequence of this principle, which has met beautiful confirmation by precision measurements at various experiments, especially at e^+e^- colliders. A characteristic prediction of the theory, the self-coupling of the gauge bosons, has also been measured and confirmed.

The Higgs mechanism, stated very simply, is the origin of mass. Without this mechanism, the masses of the quarks, leptons, and the weak gauge bosons would all be zero. These particles have mass only because the vacuum, the state of lowest energy, breaks the symmetry of the theory. In the Standard Model, this symmetry breaking is assigned to the Higgs field which interacts with, besides the gauge bosons, the quarks and leptons, and also with itself. These interactions represent new types of force which we have not observed to date.

The whole Higgs sector, including the existence of the Higgs boson, remains a theoretical hypothesis without experimental verification. It thus becomes the prime objective of energy frontier accelerators to reveal the mechanism of electroweak symmetry breaking. This will also have a strong impact on cosmology, since it is expected that there was a period in the history of the early Universe when the symmetry was restored. The phase transition may have had an important consequence to the evolution of the Universe.

Despite the lack of direct evidence, we already have a piece of information concerning the mass of the Higgs boson. Constraints derived from precision measurements of the electroweak gauge couplings are suggestive of a low mass range of 100–200 GeV. If this is so, the forthcoming experiments at TEVATRON and LHC will have a very good chance to find a signal of the Higgs boson, and even measure some of its properties.

GLC will be particularly suited for the study of Higgs physics. It will have a unique capability to access with good accuracy a wide variety of channels involving the Higgs boson. This will be essential

in order to pinpoint the mechanism of electroweak symmetry breaking and mass generation, which may not be easy at hadron machines.

It is widely accepted that the Standard Model with one Higgs boson will not be the end of the story. The huge discrepancy between the weak scale (10^2 GeV) and the gravitational Planck scale (10^{19} GeV) is difficult to maintain within the Standard Model, and new physics related to the weak scale is expected to unveil itself in the TeV energy region. Supersymmetry is a well-motivated candidate which predicts a whole spectrum of new particles with masses ranging from several hundred GeV to a TeV. Another attractive idea is the existence of large compactified extra dimensions, where the fundamental gravitational scale is taken to be close to the weak scale. Either of these scenarios, if found to be true, will induce a drastic change in our conception of matter and space-time.

New particles and interactions in these theories lead to a number of new processes with an enormous range of different signatures. The experimental environment of e^+e^- colliders is ideal to cope with often complex and sometimes elusive signals of new physics up to the kinematic reach. GLC is no exception, and it can extend our domain to the very region where new physics is expected to appear.

New physics may also reveal itself in processes involving known particles, such as the W boson and the top quark. Since these heavy particles couple most strongly with the Higgs sector, the investigation on these processes could provide information on the dynamics of electroweak symmetry breaking. In particular, these processes will be of utmost importance if no light Higgs boson is found at LHC and GLC. In this case, something is missing in our current understanding of electroweak symmetry breaking.

Last, but not least, totally unexpected signals of new physics may be observed at GLC. The e^+e^- collider has the capability to find a wide range of unexpected particles without relying heavily on the particulars of the model that is being considered. We should remember that the third generation of particles, the τ lepton, was first found in electron-positron collisions. The discovery of the charm quark was also at an e^+e^- machine.

We may thus anticipate a wealth of new findings, possibly during the first stage of GLC, with a center-of-mass energy of 500 GeV. It is also very likely that new physics will not end there. New results are bound to trigger further questions which need to be answered by experiments at higher energy. GLC is being designed with a capacity for energy upgrades to 1 TeV or higher, which will assist the exploration of physics at the TeV scale.

In this chapter we present the highlights of research at GLC. Details are given in the ACFA report [1].

2.2 Higgs Physics

The Higgs boson plays a special role in particle physics. The Higgs field is introduced to break electroweak symmetry, and all particles including the quarks, leptons, and weak gauge bosons obtain their masses from interactions with this field. The Higgs boson is the physical excitation of this field and, if discovered, will be the first spin-zero elementary particle to be observed in Nature. The interactions of the Higgs bosons with other particles are of a new type, and directly related to the mechanism of mass generation. The origin of electroweak symmetry breaking is attributed to the self-coupling interaction acting between the Higgs bosons themselves. The Yukawa interactions of the Higgs field with the quarks and leptons generate the fermion masses by symmetry breaking. The strength of the interaction is proportional to the mass of the fermion in the Standard Model, while there would be a deviation in models beyond it.

The goal of Higgs physics is to understand the dynamics of electroweak symmetry breaking and the mass-generation mechanism of elementary particles. First, we have to establish that an observed particle has the right properties for the Higgs boson, such as zero-spin and even-parity. Then, we must measure couplings with fermions and gauge bosons. The study of the Higgs sector will also provide a key to proceed beyond the Standard Model. There is a variety of models in which the Higgs sector reflects a consequence of more fundamental physics. The structure of the Higgs sector needs to be clarified as much as possible. For example, the number of Higgs fields, the possible existence of a gauge singlet field, and/or CP-violation in the Higgs interactions, need to be examined. We definitely need a “Higgs factory” with a clean experimental environment. As shown below, the GLC can serve as the best and unique facility to fully investigate the Higgs sector.

Although the mass of the Higgs boson is a free parameter, we can limit its possible range from reasonable theoretical assumptions. If we require that the Standard Model be valid up to the Planck scale ($\sim 10^{19}$ GeV), the Higgs mass should lie between 130 and 180 GeV [2]. The minimal supersymmetric standard model (MSSM) is more restrictive and requires the lightest CP-even Higgs boson mass to be below 130 GeV for a reasonable choice of supersymmetry parameters [3]. In a more general class of supersymmetric models, we may derive an upper bound on the mass of the lightest Higgs boson if we assume that the model is valid up to the grand-unification scale or the Planck scale. The bound does not exceed about 200 GeV [4]. The successful unification of the three gauge coupling constants in the supersymmetric model gives support to this assumption[5].

Experimentally, the Higgs mass is constrained by negative results of direct searches and precision electroweak measurements. At the time of this writing, the Standard Model Higgs boson mass is in the range between 114 and 193 GeV at the 95% confidence level [6].

At GLC, the production cross section of the Standard Model Higgs boson is substantial if the mass is below 200 GeV. Its discovery would require only a few fb^{-1} of integrated luminosity. In Fig. 2.1, the luminosity required for the discovery of the Standard Model Higgs boson is shown, together with the Higgs-boson invariant-mass distribution for a low luminosity case. For an integrated luminosity of

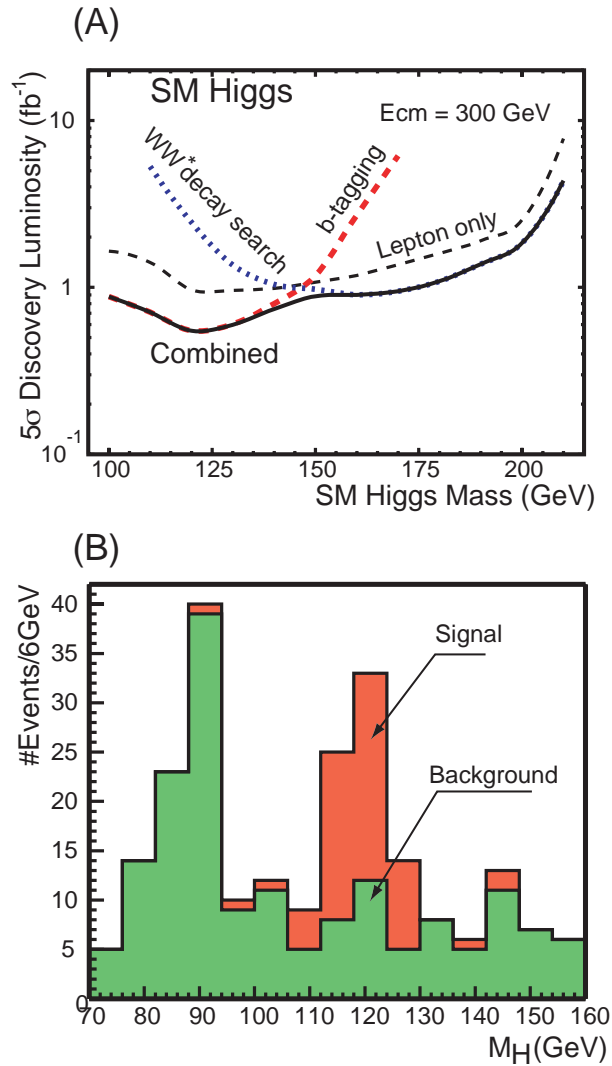


Figure 2.1: (A) Integrated luminosity required for a 5σ discovery of the Standard Model Higgs boson. (B) Invariant-mass distribution for the Higgs boson search at GLC with an integrated luminosity of 5 fb^{-1} at $\sqrt{s} = 300 \text{ GeV}$. Signals for the Standard Model Higgs boson of 120 GeV and backgrounds are shown in red and green, respectively, for combinations of the 4-jet, 2-jet + missing, and a lepton pair + $b\bar{b}$ modes.

500 fb^{-1} , about 10^5 Higgs boson events can be collected. The situation is similar in supersymmetric models. Both in the MSSM and the next-to-minimal supersymmetric standard model (NMSSM) with an extra singlet Higgs field, at least one of the CP-even Higgs bosons has a sufficiently large production cross section for the discovery [7].

With a higher luminosity, a precise determination of the Higgs mass can be done from the recoil mass distributions in the process $e^+e^- \rightarrow ZH$. The expected accuracy of the mass determination is

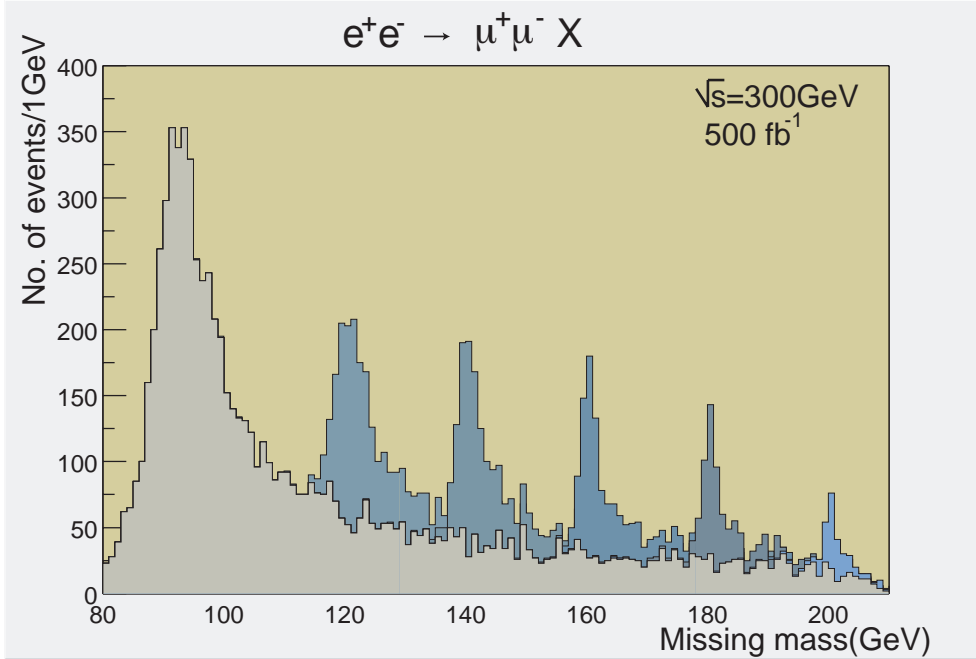


Figure 2.2: Distribution of the recoil mass of the $\mu^+\mu^-$ pair in $e^+e^- \rightarrow \mu^+\mu^- X$, normalized to 500 fb^{-1} at $\sqrt{s} = 300 \text{ GeV}$. The background from the Z^0 -pair production process, $e^+e^- \rightarrow Z^0Z^0, Z^0 \rightarrow \mu^+\mu^-$, and the SM Higgs boson signals with masses set to 120, 140, 160, 180 and 200 GeV are shown.

40 MeV for a 120 GeV Standard Model Higgs boson. A notable advantage of the e^+e^- linear collider is that the discovery of the Higgs boson is possible independently of its decay mode. The recoil mass distribution in the process $e^+e^- \rightarrow \mu^+\mu^- X$ can be used for this purpose, even if the Higgs decays to invisible particles. The expected recoil mass distribution in the $Z \rightarrow \mu^+\mu^-$ channel is shown in Fig. 2.2.

In order to confirm that an observed scalar boson is indeed the Higgs particle relevant to the electroweak symmetry breaking, we need to closely examine the properties of the observed particle. First, it is important to determine its spin and CP property. At GLC, an unambiguous determination of the quantum numbers can be made from the angular distribution in the Higgs-boson production and decay processes and the center-of-mass energy scan in the threshold region.

We then need to measure the coupling constants for Z^0Z^0H and W^+W^-H vertexes. These are the characteristic couplings which do not exist if the corresponding scalar field has no vacuum expectation value. These couplings can be determined at a few percent level for a 120 GeV Higgs boson with an integrated luminosity of 500 fb^{-1} from the production cross section through the processes shown in Fig. 2.3 [1, 8, 9]. If the measured values are consistent with the values predicted by the Standard Model, we may conclude that the observed scalar particle can in fact be interpreted as physical excitation related to the very field generating the gauge boson masses. Independent information on

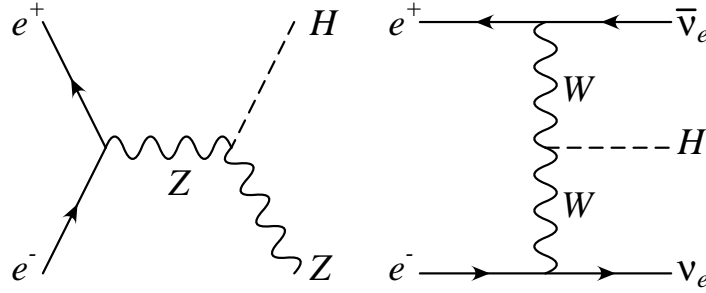


Figure 2.3: Higgs boson production processes for measurements of the Higgs-boson couplings to gauge bosons.

the W^+W^-H coupling comes from the Higgs-decay branching ratio to W^+W^- . Combining the two measurements, we should be able to determine the total width of the Higgs boson, which is one of the basic parameters of this particle. The accuracy of the total width is estimated to be 5% with an integrated luminosity of 500 fb^{-1} [1].

The Yukawa coupling of the bottom and charm quarks and the τ lepton can be determined from the corresponding decay branching ratios and the total width [1, 8, 9]. We can obtain the top quark Yukawa coupling constant by measuring the $t\bar{t}H$ production cross section. The top pair production cross section is also sensitive to the top Yukawa coupling through the virtual Higgs exchange, and indirect information on the coupling may also be obtained from its contribution to the $H \rightarrow gg$ process via the top quark loop, where g stands for a gluon. The accuracy of the coupling determination depends significantly on the mass of the Higgs boson, because the dominant decay mode differs in the lighter ($\leq 150 \text{ GeV}$) and heavier ($\geq 150 \text{ GeV}$) mass regions. In Fig. 2.4, we show the expected accuracy of these couplings for the 120 GeV Higgs boson. The expected statistical errors of the Yukawa coupling determination are a few percent, except for the charm coupling constant [1].

Double Higgs production through the $e^+e^- \rightarrow ZHH$ and $e^+e^- \rightarrow \nu\bar{\nu}HH$ processes may provide us with the first measurement of the Higgs self-coupling constant and the Higgs potential [10]. The accuracy of the self-coupling determination is shown in Fig. 2.5 [11]. For a center-of-mass energy of 500 GeV, the self-coupling constant is determined with a precision of 20% with an integrated luminosity of 1 ab^{-1} from the $e^+e^- \rightarrow ZHH$ process. If we upgrade the center-of-mass energy to 1 TeV or higher, the $e^+e^- \rightarrow \nu\bar{\nu}HH$ process becomes more important, and the expected accuracy reaches less than 10% .

A precise study of Higgs properties provides an important way to look for new physics. A deviation from the Standard Model expectation of any property of the Higgs boson must be sought. In Fig. 2.6, we show the ratio $B(h \rightarrow W^{(*)}W^{(*)})/B(h \rightarrow \tau^+\tau^-)$ in MSSM as an example [1, 12, 13] (W^* stands for a virtual W boson). This quantity is sensitive to the mass of heavy Higgs bosons, which are predicted in the model. This kind of indirect information will be important for determining the energy upgrade plan for GLC, if the heavy Higgs bosons are beyond the reach of the GLC experiment with the initial energy.

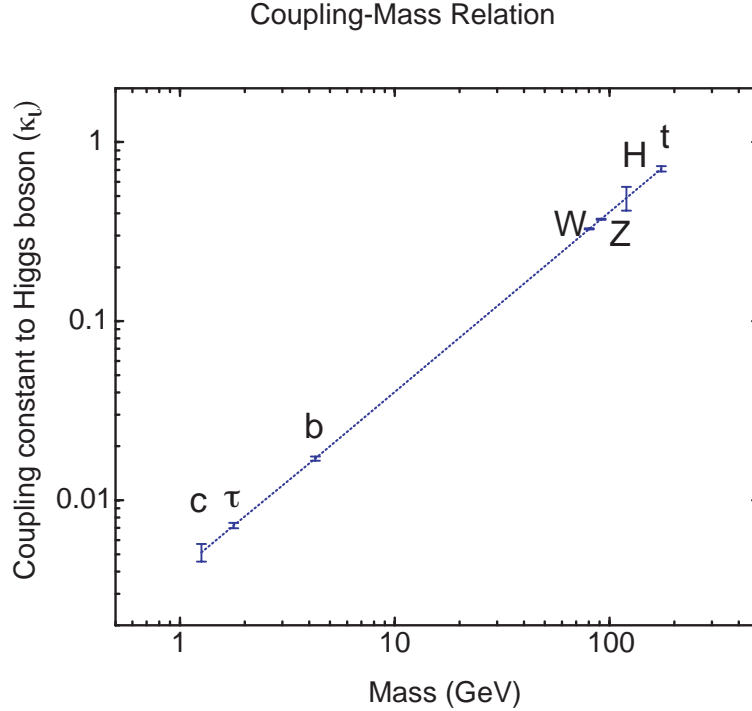


Figure 2.4: Precision of the coupling-constant determination at GLC with $\mathcal{L} = 500 \text{ fb}^{-1}$. The coupling constant, κ_i , is defined from the Higgs boson coupling to the “ i ” particle. $m_i = \kappa_i v$ holds in the Standard Model. The Higgs boson mass is taken to be 120 GeV. For the charm, tau, bottom, W and Z coupling measurements, $\sqrt{s} = 300 \text{ GeV}$ is assumed. $\sqrt{s} = 500 \text{ GeV}$ (700 GeV) is taken for the Higgs self-coupling ($t\bar{t}H$) coupling measurement.

If the energy of GLC is sufficiently large, heavier Higgs bosons may be produced directly. In the MSSM, the masses of the heavy CP-even Higgs boson (H^0), the CP-odd Higgs boson (A), and the charged Higgs boson (H^\pm) are nearly degenerate if these particles are heavier than 150 GeV. The associated production of $H^0 A$ and $H^+ H^-$ is possible if the center-of-mass energy exceeds the production threshold. The parameter space covered by various heavy Higgs production processes is shown in Fig. 2.7, where cross section contours of 0.1 fb^{-1} are given for $\sqrt{s} = 500 \text{ GeV}$ and 1 TeV. By determining their masses and couplings to fermions by measuring the branching ratios, one can test whether the observed Higgs bosons correspond to those in the MSSM. We can then derive such parameters as the vacuum mixing angle, which is one of the basic parameters of MSSM. Note that, if we can utilize the $\gamma\gamma$ option of the linear collider, the s -channel formation of A and H^0 is possible, so that the discovery mass range can be extended up to about 80% of the e^+e^- center-of-mass energy. At the $\gamma\gamma$ collider, we will be able to determine the CP property of the heavier Higgs boson and measure possible CP violation in the Higgs sector by using the polarization of the initial-state photons or decay angular distributions of the final states [14].

As discussed above, the study of the Higgs sector gives the most important physics motivation in

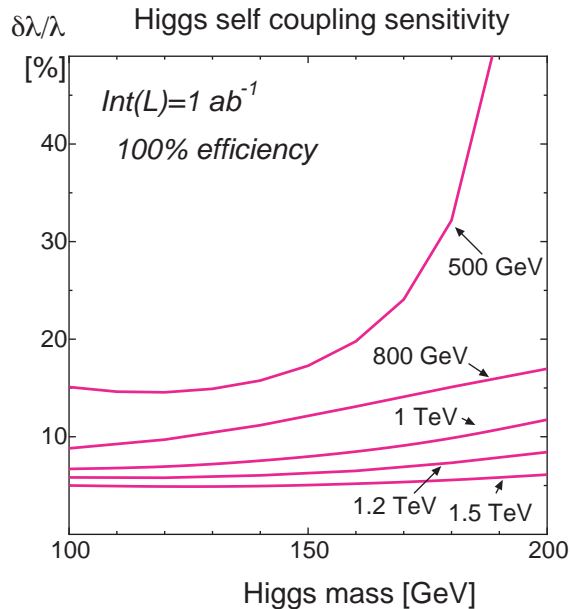


Figure 2.5: Accuracy of the triple Higgs boson coupling measurement at GLC based on the production processes of $e^+e^- \rightarrow ZHH$ and $e^+e^- \rightarrow \nu\bar{\nu}HH$. The integrated luminosity is assumed to be 1000 fb^{-1} , and 100% electron polarization is assumed for $e^+e^- \rightarrow \nu\bar{\nu}HH$. The efficiency correction is not included.

the first stage of the GLC experiment. At least one Higgs boson can be found, if the Higgs boson exists in the mass range below $\sim 400 \text{ GeV}$, which completely covers the region predicted from the electroweak measurements. The Higgs-gauge-boson coupling constant and the Higgs-fermion Yukawa coupling constants can be determined to a few to 10% level, which provides a direct grasp of the mass-generation mechanism for various elementary particles. The first non-trivial information on the Higgs potential will be obtained by measuring the Higgs self-coupling constant. From a precise study of the properties of the light Higgs boson and the search for the heavy Higgs bosons of the non-minimal Higgs sector, such as that in the MSSM, full knowledge of the Higgs sector will be obtained in the GLC experiment. This will be essential to establish the mechanism of the electroweak symmetry breaking and to look for new physics beyond the Standard Model.

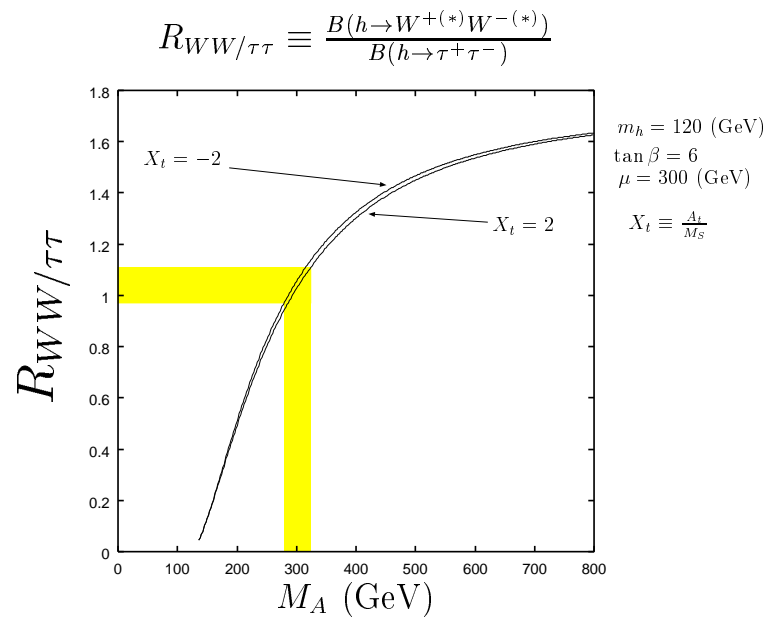


Figure 2.6: Ratio $B(h \rightarrow W^{(*)}W^{(*)})/B(h \rightarrow \tau^+\tau^-)$ for the 120 GeV lightest Higgs boson for $\tan\beta = 6$, $\mu = 300$ GeV and $X_t = \pm 2$ as a function of M_A . The shaded area shows the M_A determination from this ratio, obtained by assuming that $B(h \rightarrow W^{(*)}W^{(*)})/B(h \rightarrow \tau^+\tau^-)$ is determined with 6.7% accuracy.

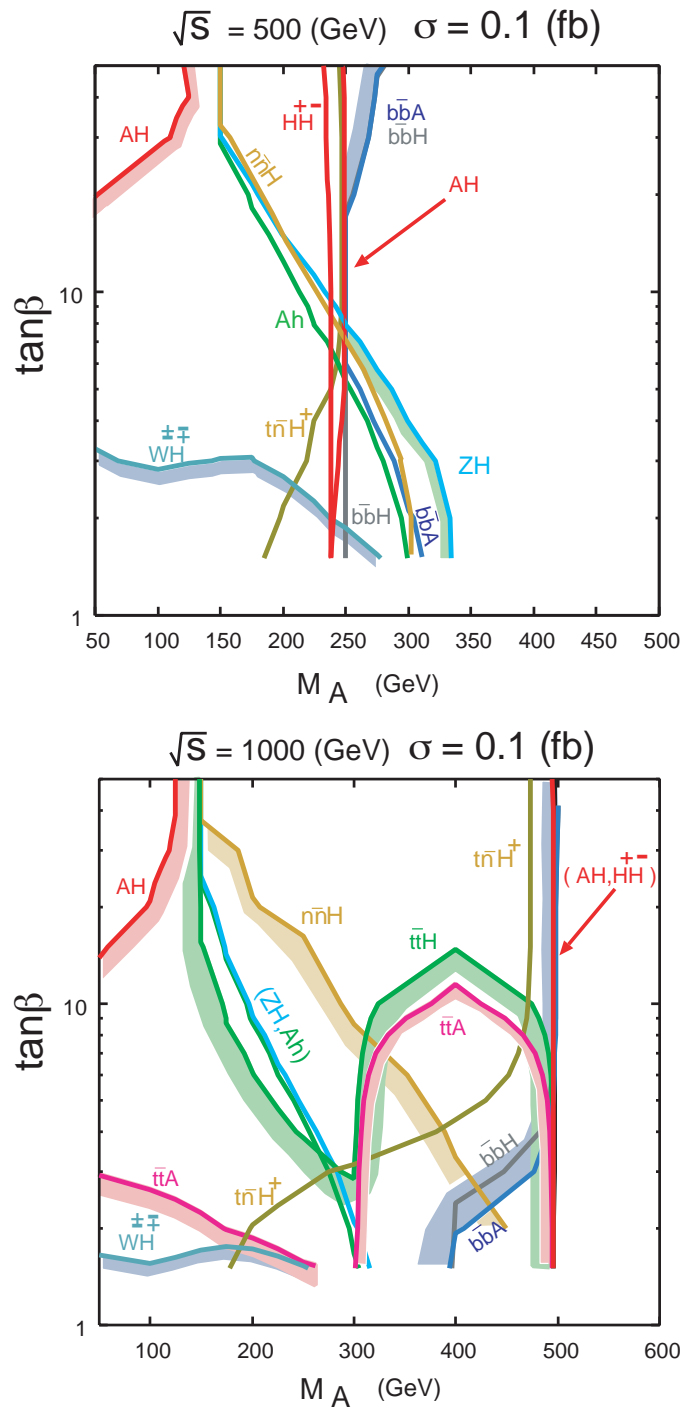


Figure 2.7: Discovery contours of various heavy Higgs production processes in MSSM. The contours of 0.1 fb^{-1} are shown in the parameter space of the ratio of two vacuum expectation values ($\tan\beta$) and the CP-odd Higgs boson mass (M_A).

2.3 Direct Signals of New Physics

As mentioned in Sec. 2.1, there are reasons to anticipate the presence of new physics beyond the Standard Model just above the electroweak scale. In many kinds of proposals for new physics, such as supersymmetry, large extra dimensions, or technicolor-type strong interactions, the appearance of new phenomena in the TeV region is common. Other new physics possibilities include new gauge bosons, such as those contained in a large unified group, like E_6 , and exotic fermions with quantum numbers different from those of quarks and leptons. Leptoquarks also tend to appear in theories in which quarks and leptons are related at some fundamental level.

GLC is capable of finding the signal of new physics for any of these scenarios, provided the energy of the machine is large enough to produce the new particles. An advantage of an e^+e^- machine is that most production and decay channels involving the new particles can be measured. This is useful in determining the basic parameters, such as the mass and spin of the new particles and their couplings. When a number of new particles are found at the same time, as is expected in supersymmetry, this is especially helpful in disentangling various signals. Beam polarization is also an important tool.

In the following, we discuss supersymmetry and a scenario with large extra dimensions in some detail. These two scenarios are particularly well motivated, and their discovery would require a drastic change in our conception of space and time. From the experimental side, they provide good case studies to illustrate the capability of the GLC experiment.

2.3.1 Supersymmetry

Supersymmetry was derived in the early 1970's by extending the four-dimensional Poincaré algebra. The symmetry requires a one-to-one correspondence between bosons and fermions. Soon after, it was realized that a remarkable cancellation occurs in the radiative correction to the scalar mass terms in theories with supersymmetry. Based on this feature, a supersymmetric extension of the Standard Model, or a grand unified theory containing it, was proposed as a solution to the hierarchy problem of the Standard Model. It was also noted that the measured value of the top quark mass naturally fits into supersymmetric models, providing a mechanism for radiatively induced electroweak symmetry breaking.

The supersymmetric extension became the prime candidate for physics beyond the Standard Model, when the three gauge coupling constants determined in the last decade turned out to meet nicely at a high energy scale in the presence of supersymmetric partners (superpartners) of the Standard Model particles. Since none of these superpartners has been observed, supersymmetry is apparently broken if it exists at all. It cannot be broken arbitrarily, however, if it is meant to solve the hierarchy problem: only soft supersymmetry breaking terms are allowed, and the mass difference between any Standard Model particle and its superpartner should not exceed $O(1)$ TeV.

In many models, some of the superpartners are within the energy reach of GLC. These supersymmetric partners include a well-motivated candidate for the dark matter, and should thus make a significant impact on cosmology if they are discovered. Furthermore, being based on an extension of the Poincaré algebra, supersymmetry has a deep connection with our space-time structure, and its breaking carries information about physics at a very high energy scale, such as the Planck scale. Discovery of the new symmetry principle and studies of supersymmetry breaking mechanism will provide us with the first realistic opportunity to probe physics at the high energy scale, and might even bring under scrutiny string theory or M-theory, or whatever else will come next. Through the new concept of the space-time established henceforth, we will touch upon fundamental questions, such as the existence of bosons and fermions, and the ultimate unification of matter, force and space-time.

As stated above, we will have a good chance to discover at least one supersymmetric particle at GLC. Although the order in which they will be discovered is model-dependent, the search methods are largely model-independent and, once we will find one supersymmetric particle, it will provide sufficient information to guide us to the discovery of the next one [15].

More important than discoveries will be precision measurements of the masses and couplings of the supersymmetric particles, since these reflect the pattern of supersymmetry breaking, which is presumably determined by some high-energy scale physics [1, 8, 9]. The clean environment of the e^+e^- collider, knowledge of the initial state momenta, and the availability of electron beam polarization will allow us to carry out these measurements in a model-independent manner [15, 16, 17], thereby allowing us to discriminate different models. This is in contrast with the LHC environment, in which we will have the copious production of colored supersymmetric particles followed by cascade decays. It is likely that the detailed information on supersymmetric particles from GLC will be essential for revealing the nature of the supersymmetry signals obtained at the LHC. Combining results of the two experiments, we will be able to illuminate the whole structure of the supersymmetry theory and answer such fundamental questions as whether or not the three gauge interactions are unified at the high-energy scale, and how and at which energy scale supersymmetry is broken [18, 19].

The discovery of supersymmetric particles will be easy at GLC as long as the collision energy is sufficiently high for pair production. The production cross sections for supersymmetric particles are typically 10 – 100 fb. The polarized electron beam is often very powerful in suppressing the Standard Model background, as shown in Fig. 2.8, yielding a very clean sample of superparticles. Using this clean sample, we can determine the mass and spin of each new particle in a model-independent fashion from the energy distributions of the decay product, the angular distributions of the production cross section, and an energy scan over the threshold region.

In Fig. 2.9, the determination of the right-handed smuon ($\tilde{\mu}_R$) and the lightest neutralino ($\tilde{\chi}_1^0$) masses is illustrated. This uses the muon energy distribution in smuon decays, in a process that the smuon decays to a muon and the lightest neutralino, which is a stable particle escaping detection. The simple two-body kinematics allows us to determine both masses from the end-points of the energy spectrum at the level of a few % with an integrated luminosity of 100 fb^{-1} . The production angular distribution in the $e^+e^- \rightarrow \tilde{\mu}_R^+ \tilde{\mu}_R^-$ process is shown in Fig. 2.10a. After background subtraction, Fig. 2.10b shows a $\sin^2 \theta$ distribution, which is characteristic of the s -channel pair production of spinless particles from

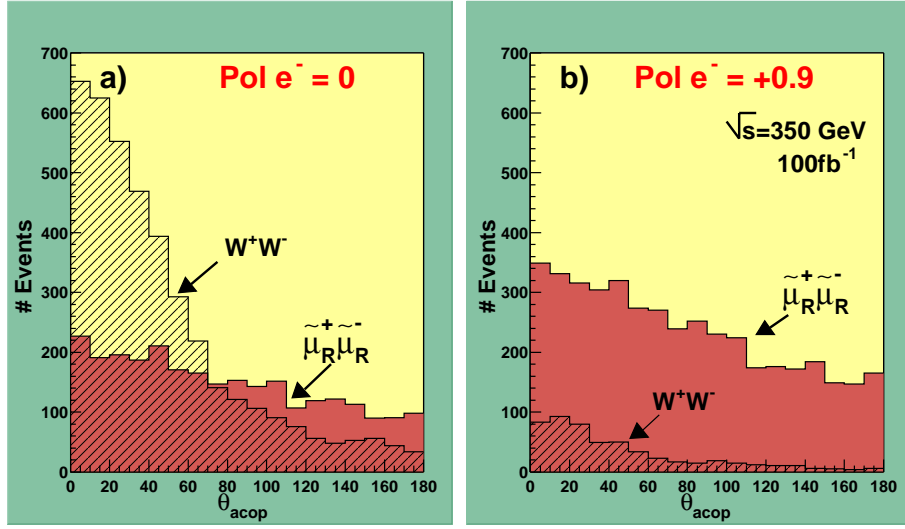


Figure 2.8: Examples of acoplanarity distributions for smuon pair productions. The Monte Carlo data correspond to an integrated luminosity of 100 fb^{-1} at $\sqrt{s} = 350 \text{ GeV}$ with (a) an unpolarized electron beam and (b) the right-handed electron beam. The solid histograms are for the signal events, while the hatched histograms are the background from W^+W^- production.

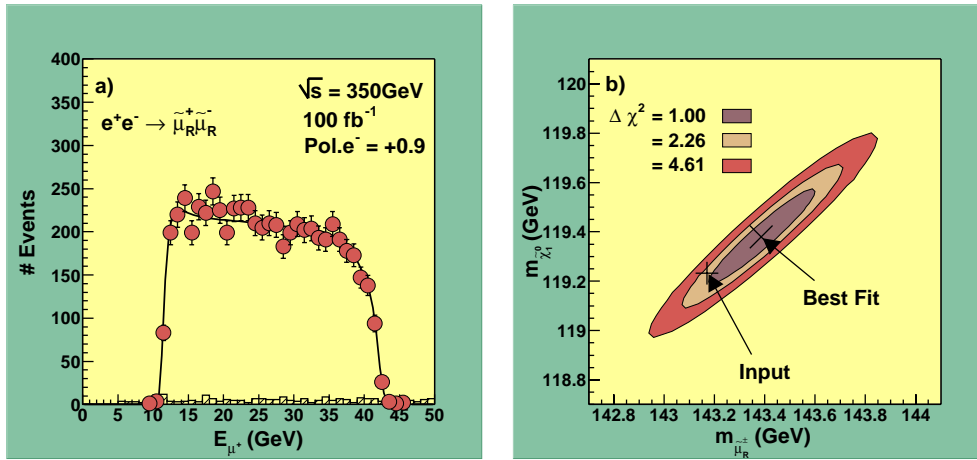


Figure 2.9: (a) Energy distribution of muons from smuon decays for the same Monte-Carlo parameters as in Fig. 2.8b. The solid line corresponds to the best-fit curve, letting $m_{\tilde{\mu}_R}$ and $m_{\tilde{\chi}_1^0}$ move freely. (b) The contours in the $m_{\tilde{\mu}_R} - m_{\tilde{\chi}_1^0}$ plane obtained from the fit to the energy distribution.

a spin 1 intermediate state. For the chargino pair-production process, $e^+e^- \rightarrow \tilde{\chi}_1^+ \tilde{\chi}_1^-$, the chargino and neutralino masses can be determined in a similar manner from the energy spectrum of the W^\pm boson in the two body decay $\tilde{\chi}_1^\pm \rightarrow W^\pm \tilde{\chi}_1^0$, as shown in Fig. 2.11.

The role of the GLC experiment will not be restricted to determining the mass and the spin of each

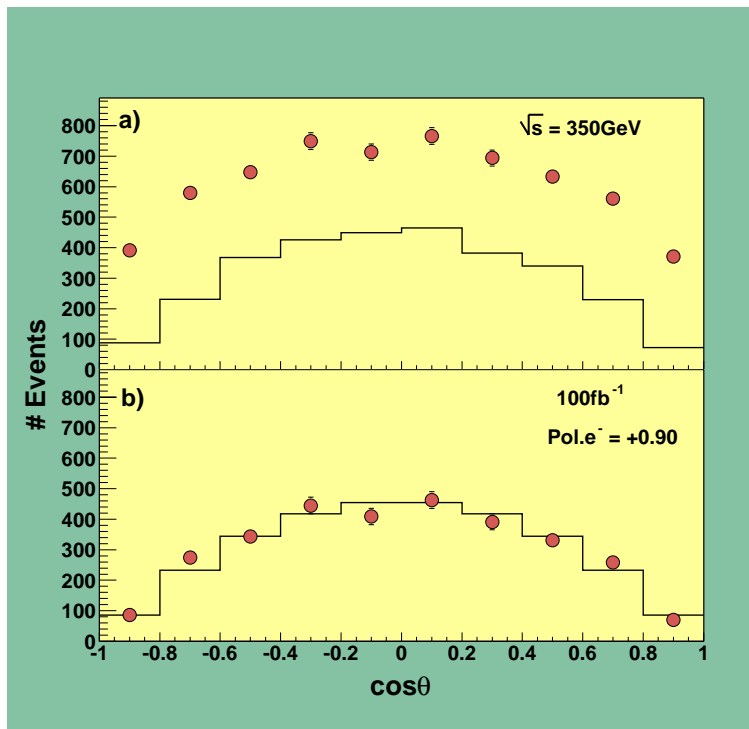


Figure 2.10: (a) Production angular distribution of $\tilde{\mu}_R^-$ with respect to the electron beam axis. The points with error bars are the distribution of the two solutions reconstructed from the selected sample corresponding to Fig. 2.9a. The histogram is the generated $\cos\theta$ distribution for the selected sample. (b) Production angle distribution after background subtraction compared with the scaled generated distribution before selection cuts. No acceptance correction is applied to the reconstructed distribution.

supersymmetric particle. From various measurements of the production cross sections, the decay branching ratios, and their angular distribution with beam polarization, we will be able to determine the form of the supersymmetric Lagrangian without relying on a particular scenario of supersymmetry breaking. This will lead us to establish a new symmetry principle of supersymmetry.

One such example is given in Fig. 2.12. Since the chargino and neutralino sectors consist of mixtures of supersymmetric partners of the gauge bosons (gaugino) and the Higgs bosons (higgsino), we need to disentangle these mixtures from various observed quantities. The $U(1)$ and $SU(2)$ gaugino mass parameters, M_1 and M_2 , can be determined from the mass and production cross section measurements of the processes $e^+e_R^- \rightarrow \tilde{e}_R^+\tilde{e}_R^-$ and $e^+e_R^- \rightarrow \tilde{\chi}_1^+\tilde{\chi}_1^-$. The electron beam polarization is essential to decomposing the mixtures. We can then perform a very interesting test of the GUT relation between the gaugino mass terms, as shown in Fig. 2.12. Combined with the gluino mass, which could be determined at LHC, we would be able to obtain important information on how the gaugino masses are generated at the high-energy scale.

Another interesting quantitative test will be available through right-handed selectron production [20].

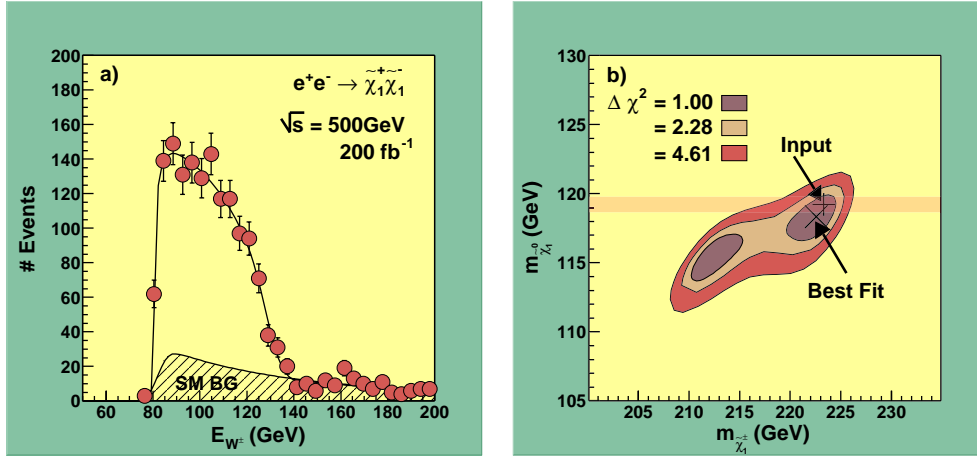


Figure 2.11: (a) Energy distribution of the final-state W^\pm from chargino decays: $\tilde{\chi}_1^\pm \rightarrow W^\pm \tilde{\chi}_1^0$ (points with error bars) after the acoplanarity angle cut at $\theta_A = 30^\circ$. The solid curve is the best-fit curve to determine $m_{\tilde{\chi}_1^\pm}$ and $m_{\tilde{\chi}_1^0}$. (b) Resultant contours from the 2-parameter fit.

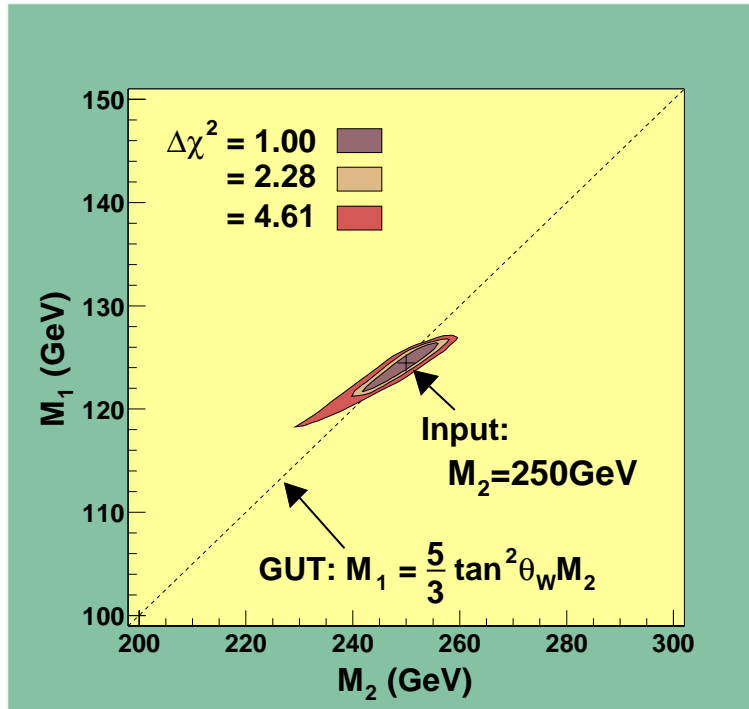


Figure 2.12: Contours of constant χ^2 in the M_2 - M_1 plane obtained from a global fit, as explained in the text. The dotted line shows the GUT relation.

This process has a t -channel bino (\tilde{B}) exchange diagram in addition to the s -channel production, and

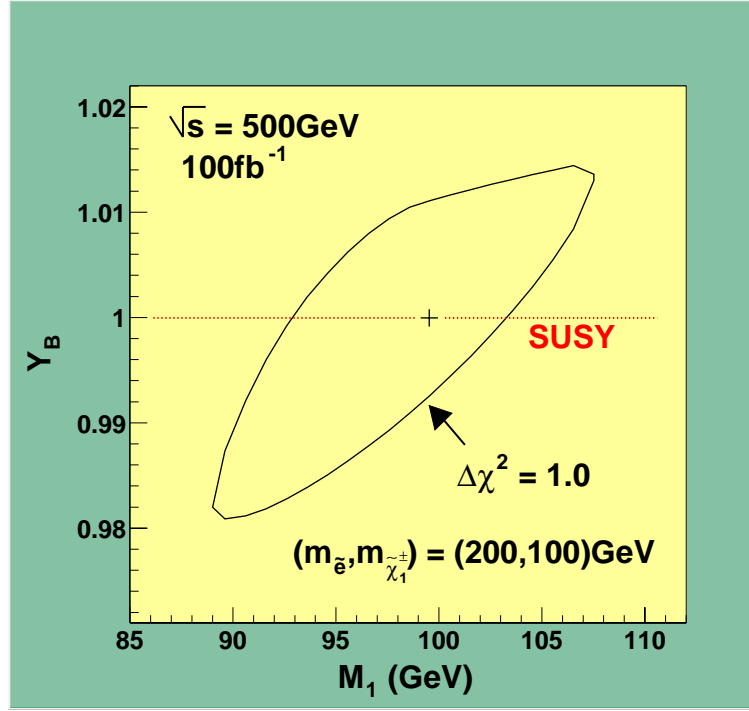


Figure 2.13: $\Delta\chi^2 = 1$ contour in the M_1 - $Y_{\tilde{B}}$ ($\equiv g_{\tilde{B}\tilde{e}_R e}/g'\sqrt{2}$) plane for pairs of \tilde{e}_R with a mass of 200 GeV generated at $\sqrt{s} = 500$ GeV with $\int L dt = 100 \text{ fb}^{-1}$. The input parameters are $\mu = 300$ GeV, $M_1 = 99.57$ GeV, and $\tan\beta = 2$.

a precise measurement of the differential cross section will provide us with the value of the bino–selectron–electron coupling constant. Since this value is related to the $U(1)$ gauge coupling constant by supersymmetry, the measurement will provide a quantitative test of the supersymmetry relation. With an integrated luminosity of 100 fb^{-1} , we can determine the coupling constant at the few % level, as shown in Fig. 2.13.

There are many other important measurements on supersymmetric particles to be made at GLC. The following is a partial list:

- Full reconstruction of the chargino mass matrix through heavy and light chargino production [21].
- Stau production and the tau polarization measurement in the stau decay to determine the stau’s Yukawa coupling [20].
- Measurement of CP violating couplings in the neutralino pair production and decay processes.
- Search for lepton flavor violation in the slepton pair production.

Whilst climbing up step by step the spectral ladder of supersymmetric particles, we will be able to

carry out these measurements model-independently thanks to the clean environment of the e^+e^- collider, the controlled initial state energy, and the availability of electron beam polarization. The detailed information on supersymmetric particles from GLC will be essential for disentangling the complex signals of supersymmetry obtained at the LHC. Combining the two experiments will enable us to grasp the whole structure of the underlying supersymmetric theory and pave the way to the ultimate unification of matter, force and space-time.

2.3.2 Large Extra Dimensions

Models with “large” extra spatial dimensions [22] have recently been proposed to provide an alternative solution to the hierarchy problem of the Standard Model. In this scenario, the existence of n -dimensional extra-space is assumed. The graviton is supposed to propagate in a $4+n$ dimensional space-time, whereas the Standard Model particles are confined on a four-dimensional “brane”. The fundamental gravitational scale should be close to the electroweak scale in order to avoid the hierarchy between the two scales. The apparent weakness of the macroscopic gravitational interaction is explained by the existence of large compactified extra spatial dimensions. In fact, the four-dimensional Planck scale, m_{Pl} , can be expressed as $m_{\text{Pl}}^2 \sim M_D^{(2+n)} R^n$, where M_D is the fundamental gravitational scale and R is the size of the extra dimensions. When M_D is on the order of 1 TeV, R varies from 0.1 mm to 1 fm for $n = 2$ to 6.

Remarkably, string theory may afford the ingredients necessary for this scenario [23], since the brane can be realized as a dynamical object. Furthermore, a string scale as low as the electroweak scale is compatible with string theory if large extra dimensions are realized by some string dynamics. Indeed, the fundamental gravitational scale may be identified with the string scale, which is the only dimensionful parameter in the theory to be fixed to reproduce the correct Planck scale.

The gravitational interaction becomes as strong as the other interactions when the energy is close to the fundamental scale. In the scenario with large extra dimensions, future collider experiments can probe the extra dimensions, or at least put a stringent limit on the fundamental scale.

One of the model-independent predictions of large extra dimensions is the existence of a tower of massive states of the graviton, namely the graviton Kaluza-Klein modes. Since the size of the extra spatial dimensions is much larger than the inverse of the fundamental mass scale, there is almost a continuous spectrum of massive gravitons at the collider energy scale.

At GLC, the direct production of a massive graviton can be searched for in the $e^+e^- \rightarrow \gamma G$ process, where G represents the graviton modes, so that the signal will be the emission of single photons accompanied by missing four-momenta. A polarized electron beam plays a crucial role in reducing the Standard Model backgrounds. The cross section for this process is proportional to $s^{n/2}/M_D^{(n+2)}$, where s is the center-of-mass energy squared and M_D is the fundamental mass scale. For $\sqrt{s} = 500$ GeV, the GLC experiment can discover direct graviton production with M_D up to 5.8 (1.7) TeV for $n = 2$ (6) with an integrated luminosity of 500 fb^{-1} . The reach can be compared with that at LHC derived from graviton-jet production, which will be in the range $M_D = 4.0 \sim 7.5$ TeV for $n = 2$ [24]. If we

observe the signal at $\sqrt{s} = 500$ GeV, we can determine the number of extra dimensions by an energy upgrade of the linear collider by measuring the energy dependence of the cross section.

A measurement of the differential cross section can also be done at the e^+e^- linear collider. This is a great advantage over the LHC, when interpreting the observed signature of the large missing momentum. The missing-mass distribution can be used for background suppression and determining the number of the extra dimensions. An example is shown in Fig. 2.14, where the fundamental scale and the number of extra-dimensions are determined by using the missing-mass distribution. The photon angular distribution carries information on the spin of the missing particle, which has to be 2 for gravitons. This is a crucial step for establishing new space-time dimensions.

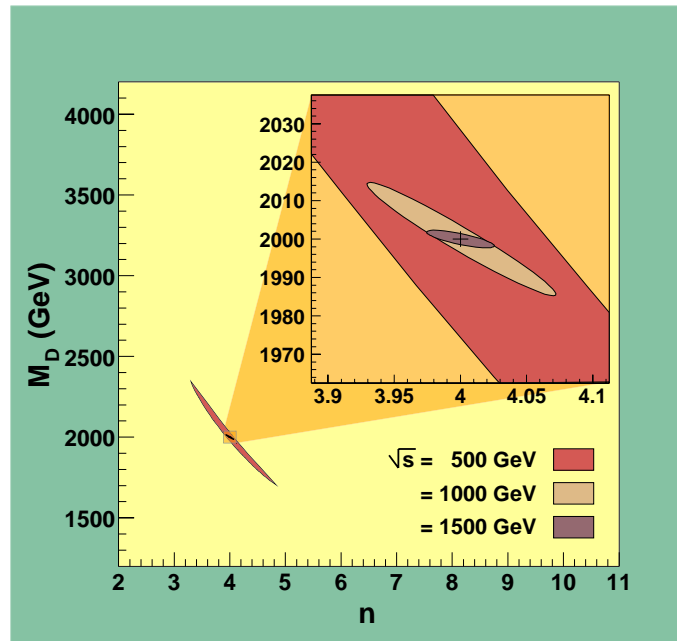


Figure 2.14: $\chi^2 - \chi_{\min}^2 = 4$ contours in the M_D vs. n plane, where n is the number of extra dimensions and M_D is the fundamental scale in $4 + n$ dimensions. Three values are taken for the center-of-mass energy at $\sqrt{s} = 500$ GeV, 1 TeV and 1.5 TeV. The integrated luminosity is 500 fb^{-1} . The input parameters are $M_D = 2$ TeV and $n = 4$. The Standard Model background due to $e^+e^- \rightarrow \nu\bar{\nu}\gamma$ is included. A cut on the minimum transverse energy of photon is set at $E_T^{\min} = 0.1\sqrt{s}$. No cut on the maximum photon energy is taken.

Graviton exchange in two-body scattering processes gives an alternative signature of the scenario of the large extra dimensions. At GLC, this can be seen as deviations from Standard Model predictions in fermion production processes, $e^+e^- \rightarrow f\bar{f}$. For $\sqrt{s} = 500$ GeV with an integrated luminosity of 500 fb^{-1} , the 95% CL search reach is about 4 TeV. The reach increases as the energy is upgraded. For instance it becomes 7 TeV for $\sqrt{s} = 1$ TeV [25].

Finally, we would like to stress that future collider experiments may reveal the nature of quantum gravity more directly, if the fundamental scale is low enough. If the energy is much larger than the

fundamental mass scale, which may be the case at LHC, a copious production of black holes may occur, followed by Hawking evaporation. However, black hole formation tends to conceal the genuine quantum gravity effects. GLC in the second phase may be in a better energy range for probing quantum gravity directly, which would open up a completely new stage of fundamental physics.

2.4 Probing New Physics through Top Quark and Gauge Boson Processes

GLC will provide a unique opportunity for precision studies of the W^+W^- and $t\bar{t}$ production. Improving the W^\pm and top quark mass determination will be important in itself, because these masses are fundamental parameters of current particle physics, and especially so, because they are essential input parameters of the precision test of the Standard Model and beyond. We can carry out measurements of anomalous coupling constants related to the gauge bosons and the top quark, including those with CP violations. In the case in which a light Higgs boson is not found at LHC and GLC, these measurements will play an important part in elucidating the correct mechanism of electroweak symmetry breaking.

2.4.1 Physics with Top Quark

The top quark is the heaviest elementary particle discovered up to now. Its mass term breaks the electroweak gauge symmetry maximally among all of the observed interactions of elementary particles. This shows that the top quark couples strongly to “something” which is condensed in the vacuum and which causes a breaking of the gauge symmetry. We thus expect that the top quark will be a key for probing the symmetry-breaking physics.

An e^+e^- collider has particular advantages in analyzing the detailed properties of the top quark, since we may make the maximal use of the spin information of the top quark in a clean experimental environment with polarized top quark samples. In the energy upgrading program of GLC, studies of the top quark will be carried out by experiments in the $t\bar{t}$ threshold region ($E_{CM} \approx 2m_t$) and in the open top region ($E_{CM} \gg 2m_t$). It is likely that the experiments in the $t\bar{t}$ threshold region will take place at an early stage of the GLC operation, and that further studies will be performed later on in the open top region.

By way of a scan of the $t\bar{t}$ production cross section in the top threshold region, we will be able to determine the top quark $\overline{\text{MS}}$ mass¹ to an unprecedented precision [26]. This precise value of the top quark mass will be indispensable when testing quantum corrections originating from the electroweak symmetry-breaking mechanism. This is because the top quark mass acts as a non-decoupling param-

¹Although there are various definitions of a quark mass, the precise determination of the $\overline{\text{MS}}$ mass is of utmost importance, since it will be used as an input parameter for predicting quantum corrections to physical observables.

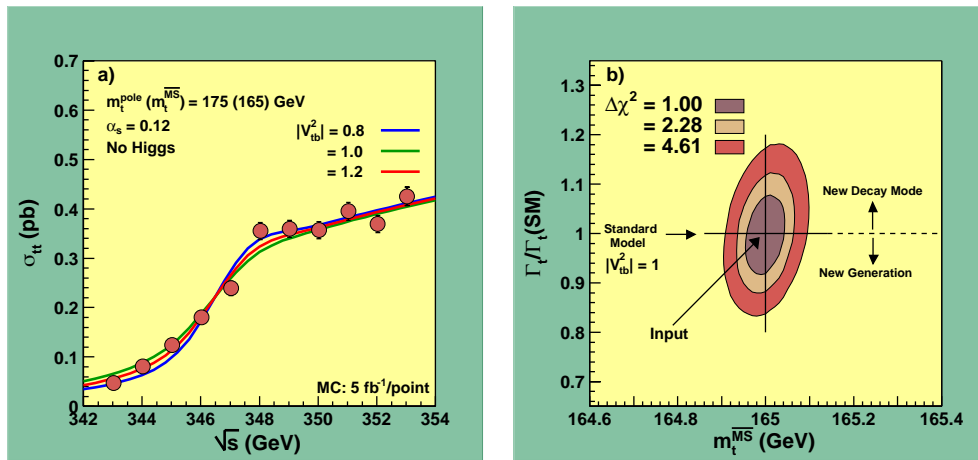


Figure 2.15: a) Dependence of the cross section on $\Gamma_t \propto |V_{tb}|^2$. A sample simulation of the energy scan is superimposed, where each point corresponds to data collected with an integrated luminosity of 5 fb⁻¹. b) The contours obtained from the fit to the data points.

eter in these quantum corrections. As an example, suppose that we will be able to measure the mass of a light Higgs boson to within 40 MeV. In order to compare the measured value of the top quark mass against the value of the Higgs boson mass predicted by the MSSM, we will need to know the top quark mass to a similar accuracy. The $t\bar{t}$ total cross section in the threshold region is shown in Fig. 2.15a. We assume an integrated luminosity of 5 fb⁻¹ at each point. From this scan we can determine the mass of the top quark with an error of 50 MeV, as can be seen in Fig. 2.15b. This will be a great improvement from the LHC experiment, where the top quark mass may be measured with 1 – 2 GeV accuracy.

The top quark decay width will also be measured most precisely over the $t\bar{t}$ threshold region. Presently the top quark width is predicted with a few % accuracy in the Standard Model as a function of the top quark mass [27]. As for the predictions beyond the Standard Model, for instance, if we include the 4th generation of fermions, the top quark width generally becomes smaller than the Standard Model prediction. On the other hand, if there are additional decay modes, such as $t \rightarrow bH^+$ or $t \rightarrow \tilde{t}\tilde{\chi}$, as in certain supersymmetric models, the top quark width becomes larger than the Standard Model prediction. It is expected that the top quark width can be measured with a few % accuracy by measuring the $t\bar{t}$ total cross section and the top quark momentum distribution in the threshold region [28, 29]. As an example, its determination from the total cross section alone is shown in Figs. 2.15a,b.

Detailed analyses of various top quark interactions will be performed both in the threshold region and in the open top region. In both regions, the clean experimental environment allows a fairly detailed reconstruction of the top quark kinematics in the production and decay chains of the top quark. In the threshold region, we may polarize the top quark close to 100%. This will be useful for decomposing its various interactions to individual components. Particularly high sensitivities to the interactions partaking in top quark decay are expected. On the other hand, experiments in the

open-top region generally have higher resolution power of the interactions involved in the top quark production processes.

Particularly interesting examples of top quark study to be performed therein are the measurements of CP violating coupling constants, such as the electric dipole moment (EDM) $ed_{t\gamma}/m_t$, the Z -EDM $g_Z d_{tZ}/m_t$ and the chromo-EDM $g_s d_{tg}/m_t$ of the top quark. These couplings are predicted to be very tiny within the Standard Model. Their detection at any near-future collider experiments will directly signal the presence of physics beyond the Standard Model. On the other hand, the presently observed baryon asymmetry in the Universe indicates the existence of a CP violation mechanism other than that of the Standard Model. It will thus be mandatory to examine CP violation in the top quark sector, which has not been tested so far. It is also important that we will be able to measure all of the above three CP violating couplings of the top quark, since the pattern of their sizes will provide valuable information on the origin of CP violation if non-zero values are found. The precision to which these couplings will be determined in the threshold region and in the open top region are shown in Table 2.1. We also compare the sensitivity expected at LHC, where only the chromo-EDM will be constrained.

		δd_{tg}	$\delta d_{t\gamma}$	δd_{tZ}
LHC	(100 fb ⁻¹)	a few $\times 10^{-3}$	-	-
e^+e^-	open top (500 fb ⁻¹)	a few $\times 10^{-1}$	10^{-2}	10^{-2}
LC	$t\bar{t}$ threshold (50 fb ⁻¹)	10^{-1}	10^{-1}	10^{-1}

Table 2.1: Sensitivity to the anomalous couplings expected at future experiments. For e^+e^- linear colliders (LC), “open top” denotes the results of studies performed at $\sqrt{s} = 500$ GeV. These results are taken from [1, 8] and references therein.

In order to compare all of the interactions of the top quark with the Standard Model predictions systematically, we will need to measure the form factors associated with all of the interactions. Simulation studies carried out so far have shown that the individual form factors can typically be measured with a few percent accuracy in the open top region [30]. As already mentioned, since the top quark couples strongly to the physics partaking in the symmetry breaking, we expect to acquire information relating to new physics from a global analysis of the top quark form factors.

As illustrated above, we will be able to carry out many important measurements, which are only possible at GLC. Although the number of the top quarks produced will be much smaller than that at LHC, GLC will play a key role in understanding the nature of the top quark and searching for new physics beyond the Standard Model through studying top quark interactions.

2.4.2 W Boson

In the Higgs mechanism of the Standard Model, the longitudinally polarized components of the physical W^\pm and Z^0 bosons conceal the hidden degrees of freedom of the Higgs field that breaks the electroweak symmetry. Therefore, a precision study of the properties of the massive electroweak

gauge bosons would yield information on the nature of electroweak symmetry breaking.

Out of the many properties of these gauge bosons, the self-couplings are amongst the least well measured. A drastic improvement will be necessary in order to be able to probe the effect of non-standard physics which enters at the loop level. The process $e^+e^- \rightarrow W^+W^-$ is suitable for this purpose, because of the strong cancellation among the diagrams involved in this process, which suppresses the Standard Model cross section. As a result, the introduction of even a small amount of non-standard interaction violating this cancellation generally leads to a sizable effect in the total cross section. If, on the other hand, the measured cross section is in agreement with the Standard Model prediction, this will impose a severe constraint on new physics.

Anomalous triple gauge boson couplings are parameterized by the coupling coefficients, $\Delta\kappa$ and λ . These are related to the magnetic dipole and quadrupole moments of the W^\pm boson. At GLC, not only the differential cross section, but the polarization of the W^\pm bosons produced and the dependence on the beam polarization can be used to achieve a precise determination of the gauge boson self-couplings. The anomalous coupling coefficients will be measured to within about 10^{-4} with an integrated luminosity of 500 fb^{-1} collected at $\sqrt{s} = 500 \text{ GeV}$. This corresponds to a two orders of magnitude improvement compared to the current values, which will allow a non-trivial test of the gauge boson couplings. As an example of a theoretical prediction, loop-induced anomalous couplings at the order 10^{-3} to 10^{-4} are expected in the Standard Model and in the supersymmetric models [31].

In addition to the W^+W^- process, there are several other gauge boson production processes, involving triple and quartic gauge boson self-couplings, available at GLC. These include the single production modes $e^+e^- \rightarrow e\nu W$ and $\nu\nu Z$, the triple production modes $W^+W^-\gamma$ and W^+W^-Z , and the final state $e^+e^-W^+W^-$ which arises via a number of multiple gauge boson interactions.

If a Higgs boson is not observed at LHC and GLC, the study of the couplings among the gauge bosons will become particularly important. This is because, in the absence of such a Higgs boson, the longitudinally polarized gauge bosons, which are remnants of the symmetry breaking Higgs field, become strongly interacting. This strong interaction between the longitudinal components of the gauge bosons may lead to p -wave resonances in the longitudinal $W_L W_L$ scattering amplitude. According to a simulation study, the sensitivity to the vector resonance can reach up to 3 TeV with data collected with an integrated luminosity of 500 fb^{-1} at $\sqrt{s} = 500 \text{ GeV}$ [1, 32].

2.5 Complementarity of LHC and GLC

Hadron machines and lepton machines are complementary to each other. The discoveries of heavy quarks and weak bosons provide some good examples. The symbol J/ψ , itself, indicates that it was discovered both in hadron and lepton machines. The bottom quark was first found in a hadron machine, but extensively studied in a lepton machine. This is also true for Z and W. The top quark was found in a hadron machine, and a lepton machine to study its properties is not yet available. In

	LHC	LC	
		500 GeV	1 TeV
Light Higgs boson (120 - 140 GeV)			
Detection	○	○	–
Width (Γ_H)	△	○	–
J^P	△	○	–
Coupling ($g_{VVH}, Y_{f\bar{f}H}$)	○	⊙	–
Top Yukawa C.C. ($Y_{t\bar{t}H}$)	△	×	○
Self-coupling (λ_{HHH})	×	△	○
500 GeV SM Higgs boson			
Detection	○	×	○
Top quark			
Δm_t	~ 1 GeV	$\lesssim 100$ MeV	–
Width (Γ_t)	×	a few %	–
Supersymmetry			
Squark mass reach	$\lesssim 2.5$ TeV	$\lesssim \sqrt{s}/2$	
Slepton/Chargino/Neutralino	Cascade decay	Pair production	
Mass measurement	○	⊙	
Proving SUSY (Spin, Coupling)	×	⊙	
Testing SUSY breaking model	○	○	
MSSM Heavy Higgs	high $\tan\beta$	$\lesssim \sqrt{s}/2$	
Indirect constraint on SUSY parameters	△	○	○
Large Extra Dimension			
KK graviton	○	△	○
Black hole production	○	×	△
Z' , KK graviton of RS model, KK mode of W and Z , etc.	Direct production	Contact interaction	
Mass reach	○	○	⊙

Table 2.2: Research potentials expected for the LHC and e^+e^- linear colliders. LHC with an integrated luminosity of $\sim 100 \text{ fb}^{-1}$ and a 500 GeV e^+e^- linear collider with $\sim 500 \text{ fb}^{-1}$ are compared. The merits of the energy extension of the linear collider to 1 TeV are shown in the column of 1 TeV LC. “Double circle”, excellent; “circle”, good; “triangle”, fair; “cross”, not useful. “–” means that this category is already fully covered at the 500 GeV e^+e^- linear collider. KK stands for Kaluza-Klein, and RS model is Randall-Sundrum model.

fact, it is one of the objectives of GLC to fill this gap.

Detailed comparisons of LHC and an e^+e^- linear collider are illustrated in Table 2.2. The comparison is categorized into several items: light Higgs boson, heavy Higgs boson, top quark, supersymmetry, large extra dimensions and exotic particles. Very generally, LHC has wider discovery range, but a linear collider is better in the detailed studies as is always the case when hadron and lepton machines are compared within a certain energy range.

In the case of the light Higgs boson, the discovery potential is more or less the same for both LHC and a linear collider. However, we definitely need a linear collider to determine its spin-parity. A linear collider also provides an excellent information on the values of most of the Yukawa couplings. This is very important, since one of the most important properties of the Higgs field is the couplings being proportional to the masses of the fermions which enter into the couplings.

The evidence of the Higgs mechanism is provided by measuring the Higgs self-coupling, and the only way to do this seems to go to a TeV linear collider to measure it with a good accuracy. One might think that a low energy linear collider could accomplish this as long as its luminosity is sufficiently high. Unfortunately, the luminosity required is beyond the current technology. It is, therefore, crucial that the potentiality to upgrade the linear collider energy be taken into account when GLC is designed.

On the items in the category of supersymmetry, one finds that the discovery range is better for LHC, if one limits the maximum energy of a linear collider at 1.5 TeV. However, here again, studies of the particle masses, spins and its couplings to other particles can be better performed in a linear collider as long as they are within its energy range. Determinations of the couplings and quantum numbers are important to prove new symmetry principles. On the other hand, a mass spectrum obtained from a combined analysis of GLC and LHC experiments is useful to discriminate various models of supersymmetry breaking. Even in the case that superpartners or heavy Higgs bosons in MSSM are beyond the energy range of the linear collider, we may be able to obtain very useful indirect evidence, just like LEP provides a possible range of mass values of the top quark and the Higgs particle. One also finds from this table that the large extra dimension can be studied in a complementary way in LHC and in a linear collider.

2.6 Summary

Energy-frontier machines provide the most effective and straightforward means to explore physics beyond the Standard Model. There are clearly many other approaches to look for new physics. Neutrino physics, B and K meson physics, and searches for proton decays and lepton flavor violating processes target different aspects of new physics. While all of these approaches are important complements to energy-frontier experiments, the study of electroweak symmetry breaking and the Higgs sector, and the direct production of new particles, require a machine with an energy which has not been attained to date. As we have just mentioned, the linear collider is an ideal and unique facility to investigate these subjects.

Energy-frontier experiments are important not only for progress in particle physics, but also for our understanding of the early Universe. Questions concerning the electroweak phase transition, the baryon number of the Universe, the dark matter and dark energy, and the inflationary universe are closely related to particle physics beyond the electroweak scale.

LHC, a hadron collider with unprecedented energy, is being constructed and will start operation within several years. Exciting discoveries in the Higgs and physics beyond it are expected to be made there. It is, however, obvious that the discovery of the Higgs boson is not the end of the story, but rather the beginning of a new era. A wealth of new physics should lie in the TeV region, and we cannot say for sure what kind of form it will take. It is just impossible to complete the physics of the Higgs sector at LHC, let alone exhaust all of these physics possibilities. In supersymmetry, LHC should be able to uncover colored superparticles utilizing its higher energy, but is not necessarily suited for uncolored particles, such as sleptons and neutralinos. A linear collider is much more capable to search for uncolored sparticles. It not only supplements the determination of the supersymmetric spectrum (toward elucidating the mechanism of supersymmetry breaking), but also supplies useful information for LHC experiments. Further, some alternative physics scenarios are extremely difficult to search at hadron machines, but within the capabilities of the electron machines. It is thus of utmost importance to start the linear collider project as soon as possible.

A possible research strategy in the first phase of GLC is as follows. First, a quick search of new particles is performed with a limited integrated luminosity of around 10 fb^{-1} at the maximum available energy. At least one Higgs boson is likely to be found and its basic properties can be determined. This luminosity is sufficient to discover supersymmetric particles, such as neutralinos, if they are within the energy reach. After this first stage, the machine energy should be optimized to maximize the production of the Higgs boson, which may be in the range between 250 and 350 GeV. A precise determination of most of the Higgs boson properties can be achieved most efficiently at this energy. Notable exceptions are the self-coupling and the Yukawa coupling with the top quark. For these studies, the machine energy should be again increased toward the maximum. On the way, an energy scan should also be performed around the threshold of the top quark pair production. In total, the investigation of the Higgs and top sectors in the first phase of GLC at center-of-mass energy of 250

– 500 GeV requires an integrated luminosity close to 1000 fb^{-1} . This luminosity is large enough for the discovery of most kinds of new particles or phenomena within the kinematic reach. Hence, an integrated luminosity of about 200 fb^{-1} per year would be sufficient to accomplish the initial physics targets within several years. One possible scenario for the GLC program is shown in Fig. 2.16 in the case that a light Higgs boson and supersymmetry will be found at GLC.

The e^+e^- linear collider can be turned to a $\gamma\gamma$ collider with minor modifications. This option is worth considering as a supplementary experiment to pursue Higgs physics. In particular, measurements of the Higgs lifetime and searches for heavier Higgs bosons in supersymmetric models can be effectively performed using the $\gamma\gamma$ option.

It is very likely that exciting new discoveries will be made during these experiments. It is also rather likely that the whole picture of the physics beyond the Standard Model will *not* become evident to us. The capability of the GLC project to extend the energy to 1 TeV or more in the second phase will be of great significance in answering new mysteries posed by new findings in the first phase.

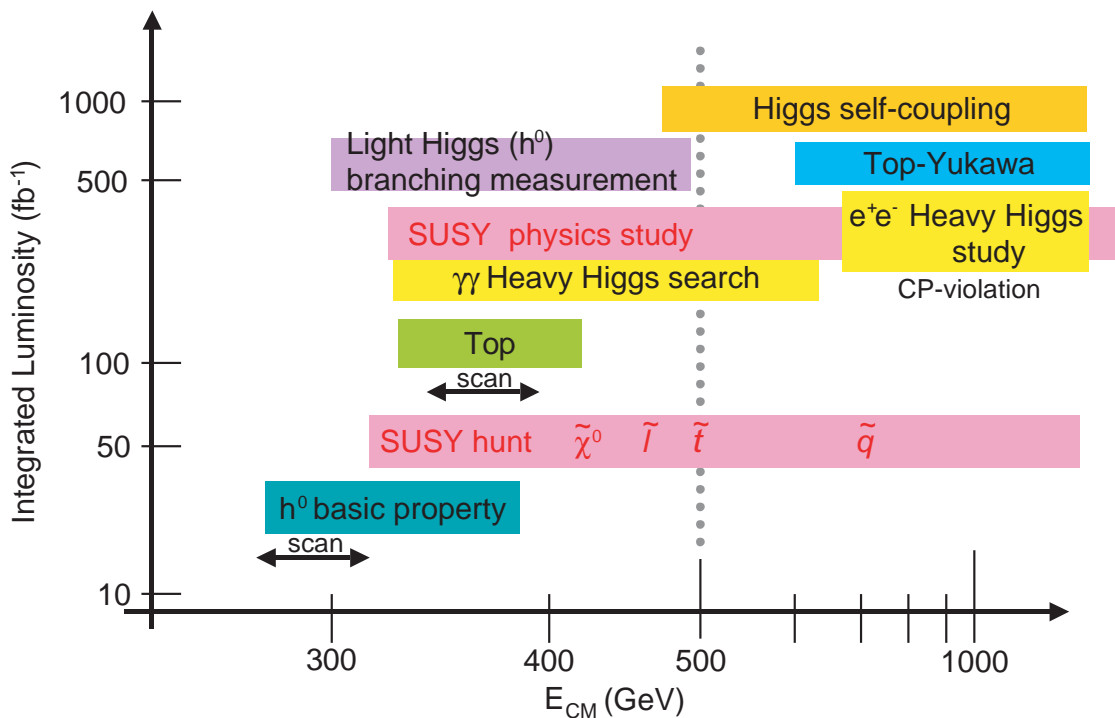


Figure 2.16: Physics covered by the GLC experiment in each stage of a center-of-mass energy and an integrated luminosity. The case with a light Higgs boson and supersymmetry is shown as an illustration.

References for Chapter 2

- [1] K. Abe *et al.* [ACFA Linear Collider Working Group Collaboration], “Particle physics experiments at JLC,” arXiv:hep-ph/0109166.
- [2] N. Cabibbo, L. Maiani, G. Parisi and R. Petronzio, Nucl. Phys. B **158** (1979) 295;
M. Lindner, Z. Phys. C **31** (1986) 295;
T. Hambye and K. Riesselmann, Phys. Rev. D **55** (1997) 7255.
- [3] Y. Okada, M. Yamaguchi and T. Yanagida, Prog. Theor. Phys. **85** (1991) 1; Phys. Lett. B **262** (1991) 54;
J. R. Ellis, G. Ridolfi and F. Zwirner, Phys. Lett. B **257** (1991) 83;
H. E. Haber and R. Hempfling, Phys. Rev. Lett. **66** (1991) 1815.
- [4] J. R. Espinosa and M. Quiros, Phys. Rev. Lett. **81** (1998) 516.
- [5] P. Langacker and M. Luo, Phys. Rev. D **44** (1991) 817;
U. Amaldi, W. de Boer and H. Furstenuau, Phys. Lett. B **260** (1991) 447.
- [6] M. W. Grünewald, Plenary talk at ICHEP02, Amsterdam, July 24-31, 2002.
- [7] J. i. Kamoshita, Y. Okada and M. Tanaka, Phys. Lett. B **328** (1994) 67.
- [8] J. A. Aguilar-Saavedra *et al.* [ECFA/DESY LC Physics Working Group Collaboration], “TESLA Technical Design Report Part III: Physics at an e+e- Linear Collider,” arXiv:hep-ph/0106315.
- [9] T. Abe *et al.* [American Linear Collider Working Group Collaboration], “Linear collider physics resource book for Snowmass 2001. 2: Higgs and supersymmetry studies,” in *Proc. of the APS/DPF/DPB Summer Study on the Future of Particle Physics (Snowmass 2001)* ed. R. Davidson and C. Quigg, arXiv:hep-ex/0106056.
- [10] M. Battaglia, E. Boos and W. M. Yao, in *Proc. of the APS/DPF/DPB Summer Study on the Future of Particle Physics (Snowmass 2001)* ed. N. Graf, eConf **C010630** (2001) E3016 ,arXiv:hep-ph/0111276.
- [11] Y. Yasui, S. Kanemura, S. Kiyoura, K. Odagiri, Y. Okada, E. Senaha and S. Yamashita, to appear in *Proc. of International Workshop on Linear Colliders (LCWS 2002)*, Jeju Island, Korea, 26-30 Aug 2002, arXiv:hep-ph/0211047.
- [12] J. Kamoshita, Y. Okada and M. Tanaka, in *Proc. of Workshop on Physics and Experiments with Linear Collider*, Morioka-Appi, September 8-12, 1995; Phys. Lett. B **391** (1997) 124.
- [13] S. Kiyoura and Y. Okada, in *Physics and Experiments with Future Linear e+ e- Colliders (LCWS 2000)*, Fermilab, Batavia, Illinois, 24-28 Oct 2000, arXiv:hep-ph/0101172.

- [14] J. F. Gunion and J. G. Kelly, *Phys. Lett. B* **333** (1994) 110;
M. Kramer, J. H. Kuhn, M. L. Stong and P. M. Zerwas, *Z. Phys. C* **64** (1994) 21; G. J. Gounaris and G. P. Tsirigoti, *Phys. Rev. D* **56** (1997) 3030 [Erratum-ibid. *D* **58** (1998) 059901];
S. Y. Choi and J. S. Lee, *Phys. Rev. D* **62** (2000) 036005;
E. Asakawa, J. i. Kamoshita, A. Sugamoto and I. Watanabe, *Eur. Phys. J. C* **14** (2000) 335;
K. Hagiwara, *Nucl. Instrum. Meth. A* **472** (2001) 12;
E. Asakawa, in *Physics and Experiments with Future Linear e^+e^- Colliders (LCWS 2000)*, Fermilab, Batavia, Illinois, 24-28 Oct 2000, arXiv:hep-ph/0101234.
- [15] T. Tsukamoto, K. Fujii, H. Murayama, M. Yamaguchi and Y. Okada, *Phys. Rev. D* **51** (1995) 3153.
- [16] J. L. Feng and D. E. Finnell, *Phys. Rev. D* **49** (1994) 2369.
- [17] J. L. Feng, M. E. Peskin, H. Murayama and X. Tata, *Phys. Rev. D* **52** (1995) 1418.
- [18] For recent review, see for instance R.M. Godbole, plenary talk given at LCWS2000, October 26-30, 2000, Fermilab, arXiv:hep-ph/0102191.
- [19] G. A. Blair, W. Porod and P. M. Zerwas, *Phys. Rev. D* **63** (2001) 017703.
- [20] M. M. Nojiri, K. Fujii and T. Tsukamoto, *Phys. Rev. D* **54** (1996) 6756.
- [21] S. Y. Choi, A. Djouadi, M. Guchait, J. Kalinowski, H. S. Song and P. M. Zerwas, *Eur. Phys. J. C* **14** (2000) 535.
- [22] N. Arkani-Hamed, S. Dimopoulos and G. R. Dvali, *Phys. Lett. B* **429** (1998) 263; *Phys. Rev. D* **59** (1999) 086004.
- [23] I. Antoniadis, N. Arkani-Hamed, S. Dimopoulos and G. R. Dvali, *Phys. Lett. B* **436** (1998) 257.
- [24] L. Vacavant and I. Hinchliffe, *J. Phys. G* **27** (2001) 1839.
- [25] J. L. Hewett, *Phys. Rev. Lett.* **82** (1999) 4765. T. G. Rizzo, *Phys. Rev. D* **59** (1999) 115010.
- [26] A. H. Hoang et al., *Eur. Phys. J. direct* **C3** (2000) 1.
- [27] M. Jezabek and J.H. Kühn, *Phys. Rev.* **D48** (1993) R1910; erratum *Phys. Rev.* **D49** (1994) 4970.
- [28] K. Fujii, T. Matsui and Y. Sumino, *Phys. Rev.* **D50** (1994) 4341.
- [29] M. Martinez and R. Miquel, hep-ph/0207315.
- [30] R. Frey, hep-ph/9606201; R. Frey et al., hep-ph/9704243.
- [31] J. Ellison and J. Wudka, hep-ph/9804322, and references therein.
- [32] M. Tanabashi, A. Miyamoto and K. Hikasa, *Proceedings of the Workshop on Physics and experiments with Linear Colliders*, Morioka-Appi, Japan, p.493, 8-12 September 1995, ed. A. Miyamoto, Y. Fujii, T. Matsui, S. Iwata.